Adaptive optics microscopy with direct wavefront sensing using fluorescent protein guide stars

Xiaodong Tao,[1,*] Oscar Azucena,[1] Min Fu,[2] Yi Zuo,[2] Diana C. Chen,[3] and Joel Kubby[1]

[1]*Jack Baskin School of Engineering, University of California, Santa Cruz, 1156 High Street, Santa Cruz, California 95064, USA*

[2]*Molecular, Cell, and Developmental Biology, University of California, Santa Cruz, 1156 High Street, Santa Cruz, California 95064, USA*

[3]*Lawrence Livermore National Laboratory, 7000 East Avenue, Livermore, California 94550, USA*

**Corresponding author: taoxd@soe.ucsc.edu*

Received May 17, 2011; revised July 20, 2011; accepted August 8, 2011;
posted August 10, 2011 (Doc. ID 147708); published August 24, 2011

We introduce a direct wavefront sensing method using structures labeled with fluorescent proteins in tissues as guide stars. An adaptive optics confocal microscope using this method is demonstrated for imaging of mouse brain tissue. A dendrite and a cell body of a neuron labeled with yellow fluorescent protein are tested as guide stars without injection of other fluorescent labels. Photobleaching effects are also analyzed. The results shows increased image contrast and 3× improvement in the signal intensity for fixed mouse tissues at depths of 70 μm. © 2011 Optical Society of America

OCIS codes: 110.1080, 010.7350, 180.2520, 180.1790, 170.3880.

Optical microscopes are essential tools in biological science. However, aberrations induced by the inhomogeneous optical properties of the sample distort the light and degrade the final image [1]. To correct the aberrations, adaptive optics (AO) have been applied in various optical microscopes [2,3]. The performance of the wavefront correction system largely depends on the wavefront measurement approach. However, wavefront sensors often require a "guide star," which is a reference point-source behind the inhomogeneous medium for measuring the shape of the wavefront. A natural or laser-generated guide star has been used in astronomy. However, it is hard to find one in biological tissues. Most of the existing AO microscopes developed so far are based on indirect methods of wavefront measurement that depend on processing of the final image [2]. The extended exposure time will cause photobleaching and limit the bandwidth for live imaging. Backscattered light has been used for direct wavefront sensing [3]. However, it is highly dependent on the backscattering efficiency of the tissue. A direct wavefront measurement method using fluorescent microspheres as guide stars has been demonstrated [4–6]. The injection of fluorescent microspheres complicates the sample preparation procedure. As an invasive method, the side effects to the functionality of the biological tissue need to be considered for live imaging.

To overcome these disadvantages, fluorescent proteins are used as laser guide stars in this Letter. We use fluorescent proteins that label particular cellular structures rather than specific layers such as the retina in the eye [7,8]. An example is green fluorescent protein (GFP), which has good photostability and high quantum yields [9]. As a noninvasive fluorescent marker, GFP has been extensively used in live cell imaging. In this Letter, a genetic mutant of GFP, yellow fluorescent protein (YFP) was investigated for wavefront measurement.

Figure 1 shows the system setup. A solid state laser ($\lambda = 515$ nm) provides the excitation light for both fluorescence imaging and wavefront sensing. The light is fed into an objective lens (×60 water objective, NA 1.2, Olympus) and scanned on the sample in a raster pattern with two galvonometer scanners (6215H, Cambridge Technology). The emission light from the YFP is divided by a beam splitter (BS). Half of the light is collected by a photomultiplier tube (PMT, H422-50, Hamamatsu). The other half of the light is used for wavefront sensing. To eliminate the intensity loss from the division of light by the BS, a switchable mirror will be included in a future system instead of the BS to maximize the signal into the PMT or the wavefront sensor. The AOs system includes a deformable mirror (DM, 140 actuators, Boston Micromachines) and a Shack–Hartmann wavefront sensor (SHWS). The SHWS is composed of a 44 element × 44 element lenslet array with a lenslet diameter of 400 μm and focal length of 24 mm (AOA Inc., Cambridge, Massachusetts) and an electron multiplying (EM) CCD camera (Cascade II, Photometrics). In order to minimize the amount of out-of-focus light that enters the SHWS, irises I1 and I2 are placed in the light path. These irises also block stray light from the DM, scanner, and lenses. The iris acts as a low pass spatial filter. However, the higher order wavefront will only give a small contribution to the overall aberration. For mouse brain tissue, the first 14 Zernike modes (third-order) contribute the most aberration. Using the method described in [10], the wavefront error with an iris can be estimated. For 50 μm thick

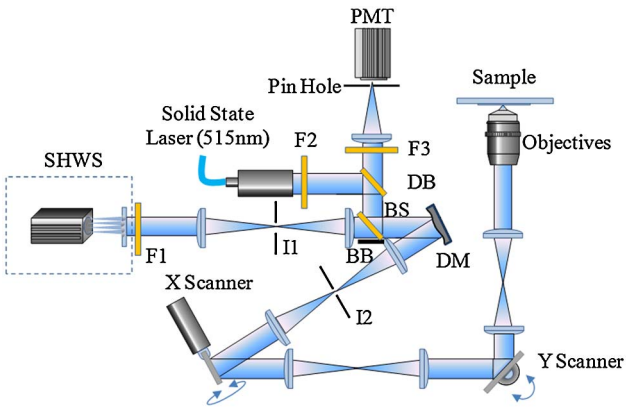

Fig. 1. (Color online) AO confocal microscope setup. DB, dichroic BS; I1 and I2, irises; F2, excitation filter; F1 and F3, emission filters; BB, beam blocker. See text for details.

mouse brain tissue, the RMS wavefront error between with and without an iris is only $0.0549\lambda(\lambda = 527\,\mathrm{nm})$ when the size of the iris is set to the diameter of the point spread function (PSF) with 80% of the encircled energy ($150\,\mu$m for I1). This setting will block 53% of the light from a plane within $1.5\,\mu$m of the focus. A cross-correlation centroiding algorithm and a fast Fourier transform reconstruction algorithm were implemented to obtain the wavefront [11,12]. To make an accurate measurement, the diameter of the guide star should be smaller than the diffraction limit of the wavefront sensor $d_{\mathrm{diffraction\_limit}}$, defined as [13]

$$d_{\mathrm{diffraction\_limit}} = 2.44\frac{\lambda}{2\mathrm{NA}}\frac{D_0}{d_l}, \tag{1}$$

where λ is the wavelength and NA and D_0 are the numerical aperture and the pupil diameter of the objective, respectively. d_l is the diameter of a lens in the Shack–Hartmann lenslet array. In our current setup, $d_{\mathrm{diffraction\_limit}}$ is equal to $5.36\,\mu$m. Because the fluorescent light from a given point is proportional to the light intensity illuminating that point, the size of the guide star is limited by the illumination PSF. The PSF is calculated from the wavefront measurement using the method described in [10]. For YFP at a depth of $70\,\mu$m, the diameter of the PSF with 80% of the encircled energy is $1.4\,\mu$m, which is small enough to be used as a guide star.

To test the system, a fixed brain tissue slice from a YFP-H line transgenic mouse was prepared. YFP is labeled on the cell bodies and protrusions of the neurons. Sample brain coronal sections ($100\,\mu$m) are mounted with antifade reagents (Invitrogen). The spherical aberration induced by the cover plate is compensated by adjustment of a correction collar on the objective lens. The approximate structure of the YFP is initially identified in the confocal image without wavefront correction. Then the laser beam is steered to the region of YFP. The YFP distribution in the background may affect the accuracy of the wavefront measurement. Similar challenges are found for nonuniformities of the sodium layer in Earth's mesosphere in astronomical laser guide stars. Nonetheless, for the mouse brain tissue studied here, the YFP in the neuron cell body with a diameter of $20\,\mu$m provides a good uniform background, where the maximum emission is from the focal plane. For other small structures, a refocusing operation is performed to achieve the best focal plane by maximizing the intensity of the Hartmann spots on the wavefront sensor. Therefore, the emission light from the focal plane makes the greatest contribution to the wavefront measurement. The DM corrects the aberration in a closed loop using the direct slope algorithm [6]. Then the corrected confocal image of the isoplanatic region [6] around the YFP guide star is captured with the optimal shape on the DM.

During the wavefront measurement, the laser focal point is fixed on the region of the YFP, which may cause photobleaching in a short amount of time if the laser power is too high. The laser power can be decreased and the exposure time of the SHWS can be increased accordingly to capture sufficient photons for the wavefront measurement before photobleaching occurs. In the current system, the laser power is adjusted manually, which takes some adjustment time. A much lower laser power is used during wavefront measurement to avoid photobleaching during the manual adjustment of the laser power. To apply higher laser power and shorter exposure times, a synchronization function between the laser power control and scanner control will be developed in the future. In this system, the laser power is turned down to 23 nW at the back aperture of the objective lens during wavefront sensing and turned up to $20\,\mu$W during confocal scanning. YFP on the dendrite and cell body of the neuron are tested as laser guide stars at depths of 25 and $70\,\mu$m, respectively, as shown in Figs. 2(a) and 2(b). The crossed lines show the location of the laser focus. The exposure time of the wavefront measurement for the dendrite and cell body is 500 and 30 ms, respectively. Because the dendrites have less YFP than the cell bodies, longer exposure times are required for accurate wavefront measurement. The wavefront measurements are shown in Figs. 2(c) and 2(d). The RMS errors are 0.17λ and 0.35λ. Photobleaching is tested for the YFP in a dendrite because it has a lower concentration of fluorophores, and thus photobleaches more quickly. Confocal images are obtained every 30 s during the exposure of the laser with 23 nW at the back aperture of the objective lens for wavefront sensing. The intensity change in the focal area is shown in Fig. 3. After the first 3 min, the intensity drops less than 10%. Considering the

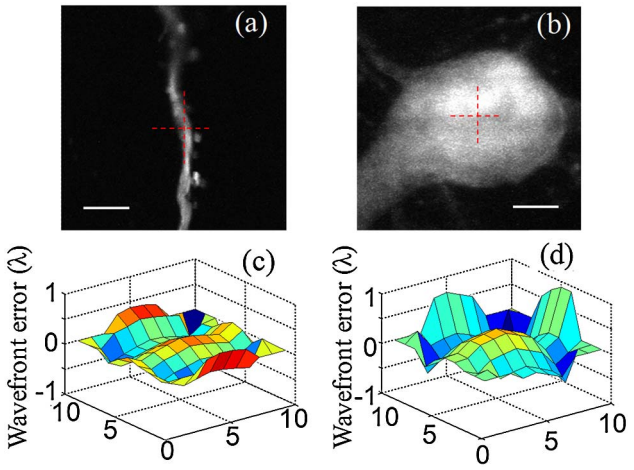

Fig. 2. (Color online) Wavefront measurements using YFP-labeled structures as guide stars. The excitation light source is focused on a cell body of a neuron in (a) and on a dendrite in (b). The scale bars are $5\,\mu$m. The crossed lines indicate the location of the focus point. The wavefront measurements are shown for a dendrite in (c) and a cell body in (d) (x, y scale in subapertures).

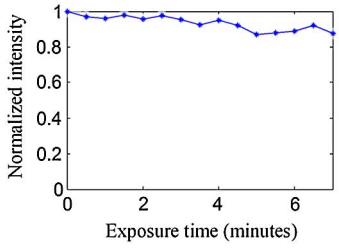

Fig. 3. (Color online) Photobleaching analysis. Normalized intensity at the focal point on the dendrite.

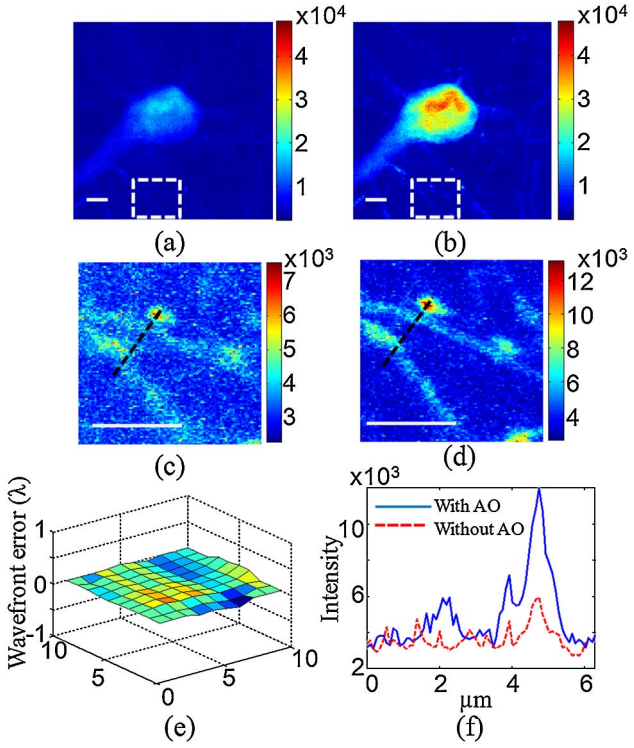

Fig. 4. (Color online) Confocal fluorescence imaging of mouse brain tissue. The maximum intensity projection image (a) before and (b) after correction. The dashed boxes indicate enlarged images (c) before and (d) after correction. (e) Wavefront error after correction (x, y scale in subapertures). (f) Intensity profiles along the dashed lines in (c) and (d). The scale bar is $5\,\mu$m.

exposure time (500 ms) for the wavefront measurement, photobleaching caused by the wavefront measurement is very limited. The measurement errors for different numbers of photons per subaperture can be measured using the method described in [14]. The EM gain setting for the EMCCD is 200×. The photons per subaperture for the two examples shown in Figs. 2(c) and 2(d) are 1950 and 2047, respectively, which produce 0.03λ in measurement error. This amount of wavefront error is small and improvements at this level will also depend on the errors caused by limitations of the DM and wavefront temporal variations. These much smaller errors for the system will be investigated in the future, but are not considered to be significant compared to the much larger wavefront corrections discussed here.

The confocal images are collected by scanning along the Z axis with a $3\,\mu$m range and a $0.15\,\mu$m step size. The final image is achieved by maximum intensity projection applied to the images. After turning on the DM, the wavefront error converges after approximately 10 iterations, which takes about 0.30 s. The YFP on the cell body was used as a guide star, which is located at a depth of $70\,\mu$m, as shown in Fig. 2(b). The RMS wavefront errors without correction and with correction are 0.35λ and 0.034λ, respectively, as shown in Figs. 2(d) and 4(e). The confocal images before correction and after correction are shown in Figs. 4(a) and 4(b). The intensity profile along the dashed lines across a dendrite and a spine is shown in Fig. 4(f). The peak intensity increases by 3×. The image of the dendrite and spines is much clearer after correction with improved contrast. The Strehl ratio is improved from 0.29 to 0.96, a significant 3.3× improvement.

To validate the proposed method, mouse brain tissues with fluorescent microspheres ($1\,\mu$m diameter, Bangs Laboratories, Inc.) are prepared. The wavefront error is corrected using the fluorescent protein first. Then the wavefront is measured again using a nearby fluorescent microsphere, which is located $3\,\mu$m from the fluorescent protein. Twenty measurements are made. The average RMS wavefront error on the fluorescent protein and microsphere are 0.0352λ and 0.0348λ, respectively, with variances of $5.9\times10^{-7}\lambda^2$ and $1.9\times10^{-7}\lambda^2$, respectively. The average RMS difference between these two methods is only 0.0272λ.

To conclude, as a noninvasive and high speed method, using fluorescent proteins for laser guide stars in AO generalizes the direct wavefront sensing method for AO microscopy, which is particularly suitable for live *in vivo* imaging.

This material is based upon work supported by the National Science Foundation (NSF) under Award No. 0852742 and the W. M. Keck Center for Adaptive Optical Microscopy at UC Santa Cruz.

References

1. M. J. Booth, Phil. Trans. R. Soc. A **365**, 2829 (2007).
2. D. Debarre, E. J. Botcherby, T. Watanabe, S. Srinivas, M. J. Booth, and T. Wilson, Opt. Lett. **34**, 2495 (2009).
3. M. Rueckel, J. A. Mack-Bucher, and W. Denk, Proc. Natl. Acad. Sci. USA **103**, 17137 (2006).
4. O. Azucena, J. Crest, S. Kotadia, W. Sullivan, X. Tao, M. Reinig, D. Gavel, S. Olivier, and J. Kubby, Opt. Lett. **36**, 825 (2011).
5. X. Tao, B. Fernandez, O. Azucena, M. Fu, D. Garcia, Y. Zuo, D. Chen, and J. Kubby, Opt. Lett. **36**, 1062 (2011).
6. O. Azucena, J. Crest, J. Cao, W. Sullivan, P. Kner, D. Gavel, D. Dillon, S. Olivier, and J. Kubby, Opt. Express **18**, 17521 (2010).
7. D. P. Biss, D. Sumorok, S. A. Burns, R. H. Webb, Y. Zhou, T. G. Bifano, D. Côté, I. Veilleux, P. Zamiri, and C. P. Lin, Opt. Lett. **32**, 659 (2007).
8. L. Diaz Santana Haro and J. C. Dainty, Opt. Lett. **24**, 61 (1999).
9. J. R. Lakowicz, *Principles of Fluorescence Spectroscopy* (Springer, 2006).
10. J. Beverage, R. Shack, and M. Descour, J. Microsc. **205**, 61 (2002).
11. S. Thomas, T. Fusco, A. Tokovinin, M. Nicolle, V. Michau, and G. Rousset, Mon. Not. R. Astron. Soc. **371**, 323 (2006).
12. L. A. Poyneer, D. T. Gavel, and J. M. Brase, J. Opt. Soc. Am. A **19**, 2100 (2002).
13. O. Azucena, X. Tao, J. Crest, S. Kotadia, W. Sullivan, D. Gavel, M. Reinig, S. Olivier, and J. Kubby, Proc. SPIE **7931**, 79310J (2011).
14. K. Morzinski, L. C. Johnson, D. T. Gavel, B. Grigsby, D. Dillon, M. Reinig, and B. A. Macintosh, Proc. SPIE **7736**, 77361O (2010).